Formation of the hematite-bearing unit in Meridiani Planum: Evidence for deposition in standing water

Philip R. Christensen and Steven W. Ruff

Department of Geological Sciences, Arizona State University, Tempe, Arizona, USA

Received 31 December 2003; revised 30 March 2004; accepted 9 June 2004; published 17 August 2004.

[1] The most plausible models for the origin and evolution of a unique geologic unit in Meridiani Planum, Mars, are low-temperature precipitation of Fe oxides/oxyhydroxides from standing water, precipitation from circulating fluids of hydrothermal origin, or the thermal oxidation of magnetite-rich ash. Analysis of Odyssey Thermal Emission Imaging System (THEMIS) infrared and visible images, together with MGS TES, MOLA, and MOC data, has provided additional insight into the Meridiani region. The hematite at Meridiani was most likely derived from a Fe oxyhydroxide precursor such as goethite, is mixed with basalt as the major component, occurs as a thin layer meters to <200 m thick, and is thermophysically distinct from units immediately above and below. Remnants of a hematite-poor unit lie directly above the hematite layer, indicating that hematite formation was sharply confined vertically. The hematite unit appears to embay preexisting channels and occurs only as outliers within closed crater basins, suggesting that it was deposited in a gravity-driven fluid, rather than as a dispersed air fall. The hematite unit lies within a topographic trough over ~3/4 of its circumference, with the remaining perimeter <150 m lower in elevation. Oxidation of ash during emplacement is unlikely given a goethite precursor and basalt as the major component. Hydrothermal alteration does not account for the confined vertical extent of the hematite layer over large distances and across disconnected outliers. The preferred model is the deposition of hematite or precursor Fe oxyhydroxides in water-filled basins, followed by dehydroxylation to hematite in low-temperature diagenesis. This model accounts for (1) the uniform deposition of a thin hematite-bearing unit over an area ~150,000 km^2 in size; (2) the transition from hematite-rich to hematite-poor units over less than ~10 m vertical distance; (3) the distinct differences from the underlying layers; (4) goethite as the precursor to hematite; (5) the embayment relationships; (6) the occurrence of remnants of the hematite-bearing unit in isolated craters surrounding the main deposit; (7) the lack of other hydrothermal minerals; and (8) the presence of coarse-grained, low-albedo basalt, rather than ash, as the major component. The occurrence of unweathered olivine, pyroxene, and feldspar throughout the equatorial region provides strong evidence that extensive aqueous weathering has not occurred on Mars. Thus the presence of a small number of bodies of standing water appears to represent brief, localized phenomena set against the backdrop of a cold, frozen planet. *INDEX TERMS:* 5410 Planetology: Solid Surface Planets: Composition; 6225 Planetology: Solar System Objects: Mars; 5464 Planetology: Solid Surface Planets: Remote sensing; 3672 Mineralogy and Petrology: Planetary mineralogy and petrology (5410); *KEYWORDS:* hematite, Meridiani, standing water

Citation: Christensen, P. R., and S. W. Ruff (2004), Formation of the hematite-bearing unit in Meridiani Planum: Evidence for deposition in standing water, *J. Geophys. Res.*, *109*, E08003, doi:10.1029/2003JE002233.

1. Introduction

[2] The Meridiani Planum region, centered near 0°N, 0°E, has received special attention following the discovery of gray crystalline hematite from thermal infrared spectra measured by the Mars Global Surveyor (MGS) Thermal Emission Spectrometer (TES) instrument [*Christensen et al.*, 2000b, 2001; *Morris et al.*, 2000; *Hynek et al.*, 2002; *Lane et al.*, 2002; *Arvidson et al.*, 2003; *Lane et al.*, 2003]. This irregularly shaped unit, centered at ~357°E and 2°S and spanning ~500 km in the E-W direction and ~300 km N-S, represents the first rock stratigraphic unit mapped on Mars on the basis of the combination of mineralogic and stratigraphic information and was named the Meridiani Formation. The likely role of water in the formation of the hematite deposit [*Christensen et al.*, 2000b, 2001; *Hynek et al.*, 2002; *Lane et al.*, 2002; *Arvidson et al.*, 2003; *Newsom et al.*, 2003] led to the selection of this site for in situ exploration by the Mars Exploration Rover

0148-0227/04/2003JE002233$09.00

Opportunity. The Meridiani hematite occurs in a primarily basaltic unit that is exposed at the top of a sequence of layered, easily eroded rocks that are stratigraphically above and postdate the ancient cratered terrain [*Presley and Arvidson*, 1988; *Edgett and Parker*, 1997; *Christensen et al.*, 2000b, 2001; *Hynek et al.*, 2002; *Arvidson et al.*, 2003].

[3] The hematite-bearing unit in Meridiani has a smooth, flat surface and average rock abundance of ~7% that provides a safe surface upon which to land and conduct rover operations. The TES-derived thermal inertia values range from ~170 to 240 (units of J m^{-2} $s^{-1/2}$ K^{-1} used throughout), corresponding to an average unconsolidated particle size of ~65–300 μm [*Presley and Christensen*, 1997]. Within the Rover landing ellipse the albedo ranges from ~0.14 to 0.19 and the dust cover index (DCI) ranges from ~0.96 to 0.98 [*Ruff and Christensen*, 2002]. These thermophysical properties indicate that Meridiani is a location with little dust accumulation, with a surface that both is trafficable and will have abundant coarse particles.

[4] Several authors have investigated the Meridiani region using data from the TES, the MGS Mars Orbiter Laser Altimeter (MOLA), and the MGS Mars Orbiter Camera (MOC) [*Christensen et al.*, 2000b, 2001; *Hynek et al.*, 2002; *Lane et al.*, 2002; *Arvidson et al.*, 2003]. The Mars Odyssey Thermal Emission Imaging System (THEMIS) cameras have imaged this region extensively at 100 m per pixel in day (Figure 1) and night (Figure 2) infrared and 18 m per pixel in the visible [*Christensen et al.*, 2003a], providing significantly improved coverage and context imaging for geologic analysis. In this paper we incorporate these observations with previous ones to provide additional insights into the physical properties and regional morphology of the hematite-bearing unit and its surroundings in order to further constrain the geologic history of the Meridiani region.

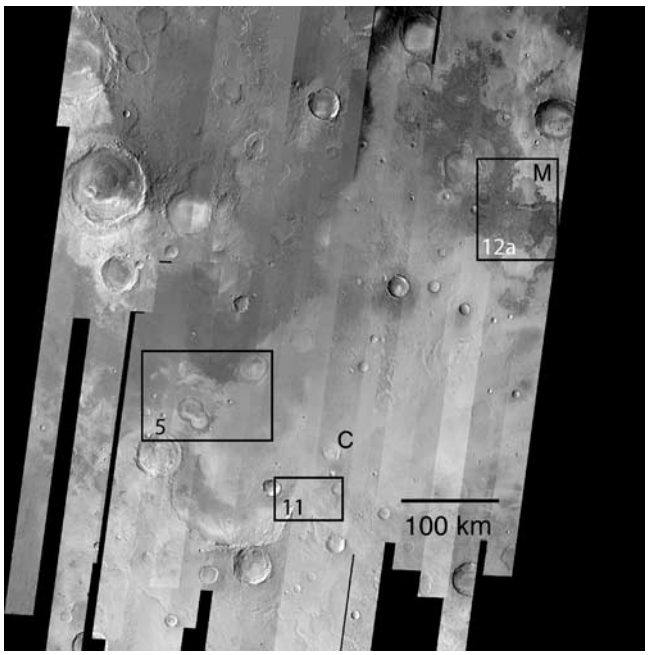

Figure 1. Mosaic of daytime THEMIS infrared images of Meridian Planum. This mosaic covers the region from 5°S to 5°N and 350° to 360°E. The images were collected at local times from 15.5 to 17.5 H (24 H equal one Martian day). The resolution of each IR image is 100 m per pixel. The locations of features mesa (M) and crater (C) discussed in the text and in Figure 3 are shown for reference, located at the lower left corners of their respective letters. The individual images were normalized prior to mosaicking to reduce temperature differences due to seasonal and local time variations. The outlines of Figures 5, 11, and 12a are shown for reference.

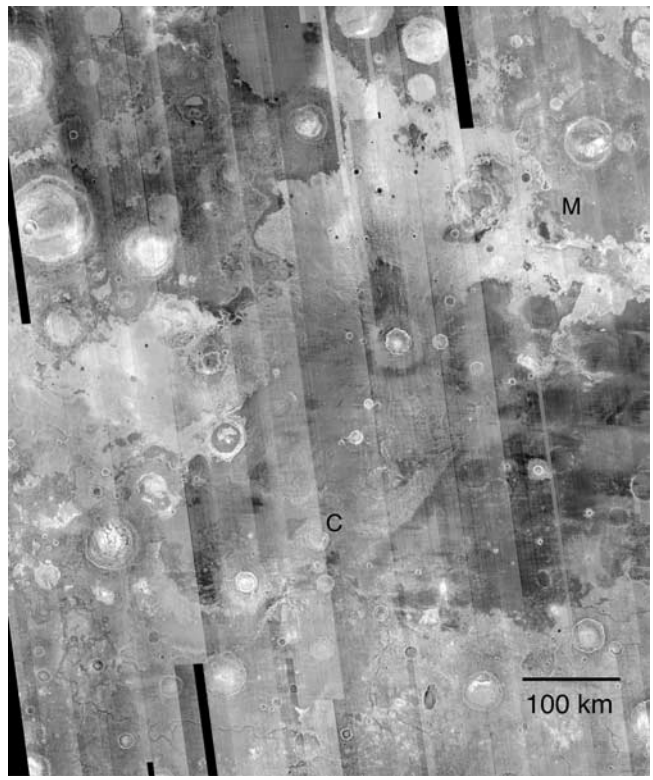

Figure 2. Mosaic of nighttime THEMIS infrared images of Meridian Planum. This mosaic covers the region from 5°S to 5°N and 350° to 360°E. The images were collected at local times from 3.5 to 5.5 H (24 H equal one Martian day). The resolution of each IR image is 100 m per pixel. The locations of features mesa (M) and crater (C) discussed in the text and in Figure 3 are shown for reference, located at the lower left corners of their respective letters. The individual images were normalized prior to mosaicking to reduce temperature differences due to seasonal and local time variations.

2. Observations and Interpretations

2.1. Composition

[5] The abundance of hematite in the surface materials of the hematite-bearing Meridiani Formation (Unit P2 of *Hynek et al.* [2002]; Ph of *Arvidson et al.* [2003]; hereinafter referred to as Ph) has been determined using linear deconvolution of TES spectra [*Ramsey and Christensen*, 1998; *Bandfield*, 2002] to vary from ~5% to ~20%. The derived hematite abundance depends on the particle size of the hematite end-member used in the deconvolution model

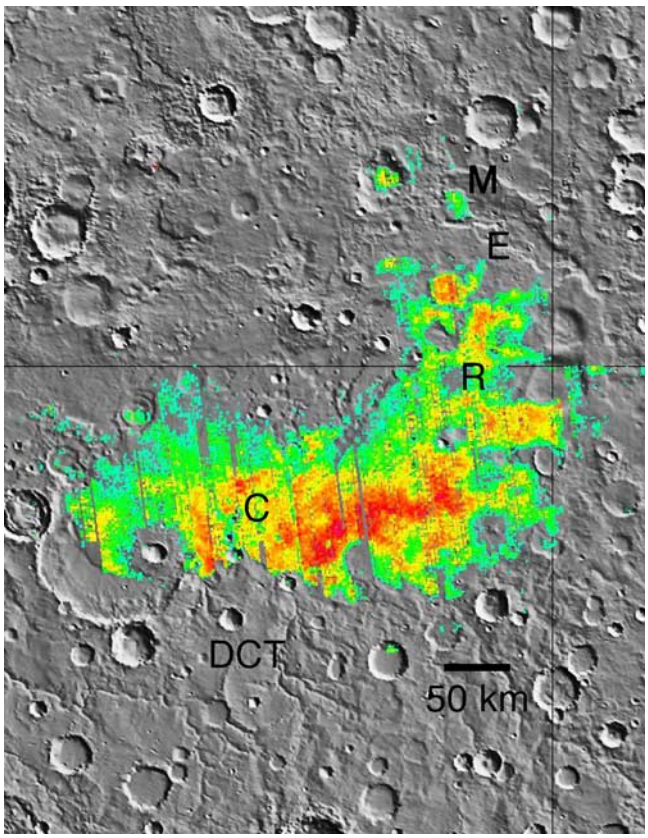

Figure 3. Occurrence of hematite-bearing units in Meridiani Planum. The hematite abundance derived from TES data is shown superimposed on a shaded relief image derived from MOLA data [*Smith et al.*, 2001]. The TES hematite abundances vary from ~5% (blue) to ~20% (red). Data where the hematite spectral signature was less than a detectable limit of ~5% have been set to zero (transparent). The positions of specific areas rise (R), mesa (M), and crater (C) discussed in the text are located at the lower left corners of their respective letters. The location of representative occurrences of Etched (E) and dissected cratered terrain (DCT) of *Arvidson et al.* [2003] are indicated by letters. A conservative lower hematite detection limit was applied to this figure to emphasize locations with strong hematite signatures. Vertical and horizontal lines are at 0° longitude and 0° latitude, respectively.

because of the variation in spectral band depth with particle size. However, an upper limit of hematite abundance can be determined using the depth of the silicate spectral feature from 8 to 14 μm. The emissivity of this feature is 0.955 [*Christensen et al.*, 2001] compared to a value of 0.945 observed in TES spectra for regions mapped as 100% basalt [*Christensen et al.*, 2000a]. Thus the silicate band is reduced by only 20%, providing the upper limit on hematite where it is most abundant. Figure 3 shows a map of hematite abundance derived from TES spectra, scaled to give a maximum abundance value of 20%.

[6] Laboratory thermal emission measurements of hematite samples show variations in spectral properties for samples derived from different precursor minerals and by different processes [*Glotch et al.*, 2004]. Hematites derived from high-temperature oxidation of synthetic magnetites provide a poor fit to the TES spectra from Meridiani, while hematites derived by lower-temperature (~300°C) dehydroxylation of synthetic goethite are an excellent match to the TES spectra [*Glotch et al.*, 2004]. Natural hematite samples that provide good spectral matches to the TES spectra also appear to have been derived from goethite precursors on the basis of XRD and Mössbauer characterization [*Glotch et al.*, 2004]. The lowest temperature at which goethite converted to hematite under dry laboratory conditions in the experiments of Glotch et al. was 300°C. However, it has been shown experimentally that under wet conditions, goethite will convert to hematite within weeks at 100°C [*Tunell and Posnjak*, 1931], and *Berner* [1969] calculated that the maximum temperature at which goethite is thermodynamically stable relative to hematite plus water is ~40°C.

[7] An atmospherically corrected surface spectrum of the hematite-bearing surface is shown in Figure 4. This spectrum closely resembles the spectrum of typical Syrtis Major basalt [*Christensen et al.*, 2000a; *Bandfield et al.*, 2000] once the hematite spectral contribution has been subtracted (Figure 4). The basalt-like shape of TES spectra from Meridiani, along with the relatively low albedo (0.14–0.18) and dust index [*Ruff and Christensen*, 2002], provides strong evidence that coarse-grained (≥~100 μm), dust-free basalt is the major component in this region. No minerals other than hematite and the plagioclase, pyroxene, and olivine found in typical Martian basalts [*Christensen et al.*, 2000b; *Bandfield*, 2002] have been identified in Ph.

[8] The abundance of hematite currently exposed at the surface does not show any systematic variation across the deposit (Figure 3). Similar, high abundances occur in the eastern, central, and far northern portions of the unit,

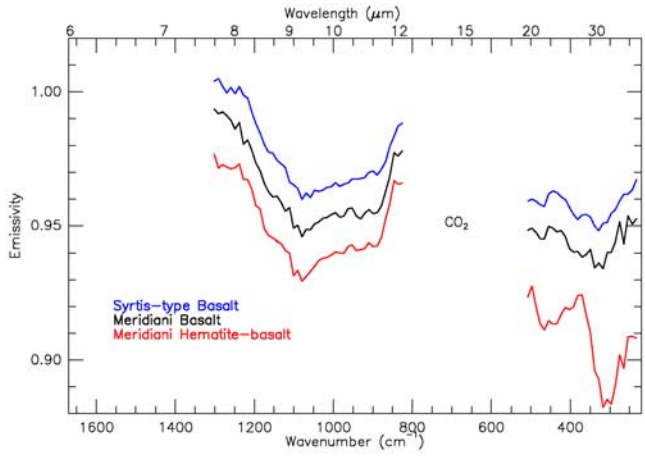

Figure 4. Comparison of atmospherically corrected TES spectra of Meridiani Planum and Syrtis-type (Type I) basalt. The red spectrum is an average of 30 TES spectra from orbit 5499 following deconvolution using the 7 TES surface and atmosphere end-members [*Bandfield et al.*, 2000]. The hematite component has been subtracted from the red spectrum to produce the black spectrum, revealing that the nonhematite component of Meridiani Planum is remarkably similar to Syrtis-type basalt.

and moderate abundances occur near the southwestern margin. There is no strong correlation with elevation derived from the Mars Global Surveyor MOLA experiment [e.g., *Smith et al.*, 2001]. Regions of high hematite abundance at −2.5°S between 354.2° and 358.7°E (Figure 3) vary in elevation from −1550 to −1300 m, and local variations of ∼100 m over 25 km distance show no significant variation in hematite abundance.

[9] In summary, the hematite at Meridiani varies in abundance from 0 to 20%, was most likely derived from a Fe oxyhydroxide precursor such as goethite, shows no coherent spatial variation in abundance or spectral character, and is mixed with a low-albedo, plagioclase/pyroxene/olivine basalt as the major component.

2.2. Thermophysical Properties

[10] The THEMIS daytime temperature images of the Meridiani region (Figure 1) show large variations that are due to solar illumination effects on topography and the thermophysical properties of thermal inertia and albedo [*Christensen et al.*, 2003a]. Local temperature variations associated with variations in thermal inertia are among the largest observed on the planet [*Christensen et al.*, 2003a]. The THEMIS nighttime temperatures (Figure 2) also show significant differences that correlate with the daytime patterns and are due to thermal inertia variations.

[11] A comparison of the distribution of hematite abundance (Figure 3) and the THEMIS mosaic reveals a close correlation between the hematite-bearing unit and surfaces that appear uniform and relatively warm (bright) in the daytime mosaic. This correlation is especially apparent along the northwest margin of Ph, where the hematite-bearing unit occurs in isolated patches associated with filled craters and intercrater mesas (Figure 5).

[12] The hematite abundance along the margins of the hematite-bearing unit drops from detectable to nondetectable levels across neighboring TES pixels spaced 3 km apart (Figure 3) [*Christensen et al.*, 2001]. This abrupt change in hematite abundance correlates with the change in morphology between the layered unit Ph and the dissected ancient cratered terrain to the south (unit DCT of *Arvidson et al.* [2003]) and the etched surface to the north (unit E of *Arvidson et al.* [2003]) (Figure 3). No hematite is detected away from Ph.

[13] Surfaces of Ph that contain hematite have been determined from THEMIS nighttime IR images to be ∼6–8 K colder (∼192 K versus ∼198 K) at night than units that are stratigraphically lower (Figure 2). These data were taken at 3.1 H (24 H equals one Martian day), aerocentric longitude (L_s) of ∼345°. These temperature differences correspond to differences in thermal inertia of 80–100 [*Fergason and Christensen*, 2003]. The thermal inertia of Ph derived from TES data [*Mellon et al.*, 2000; *Arvidson et al.*, 2003] ranges from ∼170 to 240, corresponding to a grain size of ∼65–300 μm, assuming well-sorted, unconsolidated spheres [*Presley and Christensen*, 1997].

[14] The sharp compositional boundary and particulate nature of the uppermost surface of Ph indicate that the hematite-bearing unit is covered with loose material that has been derived from an underlying, in-place rock unit [*Christensen et al.*, 2001]. As this rock unit disaggregates, the hematite-bearing component either is too coarse to be transported by the wind or becomes fine grained enough to be widely dispersed in suspension.

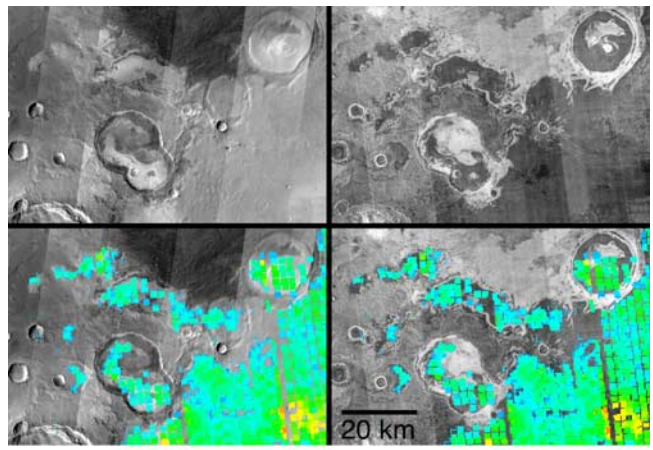

Figure 5. Hematite occurrence in series of outliers to the northwest of the main Ph unit. The hematite abundances were derived from TES and vary from ∼5% (blue) to 20% (red). The TES data are superimposed on mosaics of day (left column) and night (right column) THEMIS infrared images. The hematite-bearing materials have similar thermal properties. Seen at THEMIS resolution, these materials occur only in the uppermost layer of the stack of layered materials that form these outliers of Ph. The two major outliers in this region occur within a double crater and on a circular mesa interpreted to be the remnant floor of a crater whose walls have been completely removed. The lower hematite abundance threshold is slightly lower than in Figure 3 to emphasize the strong correlation between morphology and hematite occurrence.

[15] Preliminary mapping of this area has not revealed any overall correlation of hematite abundance with the thermal inertia properties of Ph. However, locally, the contacts between thermal units correlate with variations in hematite abundance (Figures 2 and 3), possibly indicating subtle differences between different stratigraphic layers.

[16] Unit Ph has a lower thermal inertia than the etched unit E on which it was deposited [*Hynek et al.*, 2002; *Arvidson et al.*, 2003]. The partially exhumed craters and intercrater mesas on the western margin of Ph (Figure 5) provide additional insights into the nature of Ph itself. Eroded portions of Ph in this region show that the materials within Ph that underlie the exposed hematite unit have higher thermal inertia (relatively warm at night and cold in the day) than the uppermost layer of Ph (Figure 5). This observation indicates that the uppermost portion Ph is either less indurated or erodes to less consolidated material than the materials below. This lower component of Ph is layered at THEMIS visible image scale and has a significantly different morphology than the etched unit E. We interpret these relatively high-inertia layers to be a subunit in Ph that lies below the hematite-bearing unit. These observations suggest that the hematite layer itself is a thin unit at the top of Ph.

[17] A relatively bright layer can be seen immediately below the uppermost dark unit, where it is exposed in the walls of impact craters. This bright unit is seen in craters as

small as ~500 m in diameter in the vicinity of the MER-B landing ellipse (Figure 6). These craters are only ~20 deep, indicating that the bright layer is <20 m below the surface. A similar bright unit is found several tens of meters below the surface in the northeastern portion of Ph, where it is exposed along the steeply eroded margin of Ph and in the walls of two impact craters (Figure 7). The thickness of the Ph unit above the Etched unit is several hundred meters (see below), so this bright unit appears to lie within Ph. Exposure of this subunit, rather than unit E as suggested by *Arvidson et al.* [2003], may produce the variation in albedo and thermal properties seen within the MER landing ellipse.

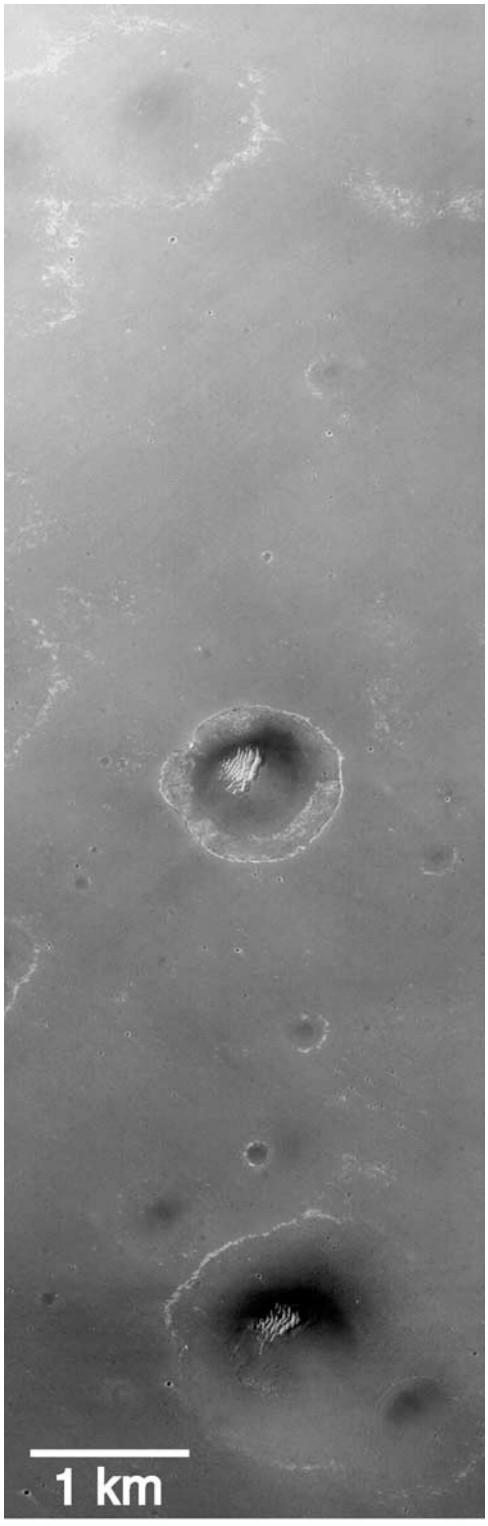

Figure 6. High-resolution MOC image (E01203255) (M. C. Malin et al., E12-03255, Malin Space Science Systems Mars Orbiter Camera Image Gallery, http://www.msss.com/moc_gallery/, 2002) of the relatively bright layer immediately below the hematite-bearing upper layer of Ph within the MER-B landing ellipse. This unusual unit appears to lie less than several tens of meters below the surface throughout this region. It is seen exposed in the walls of craters <500 m in diameter that are <~20 m deep and is interpreted to be a subunit within Ph. Image is ~3 km wide and ~10 km long, centered near 354.1°E, −1.9°S with a resolution of 3 m per pixel.

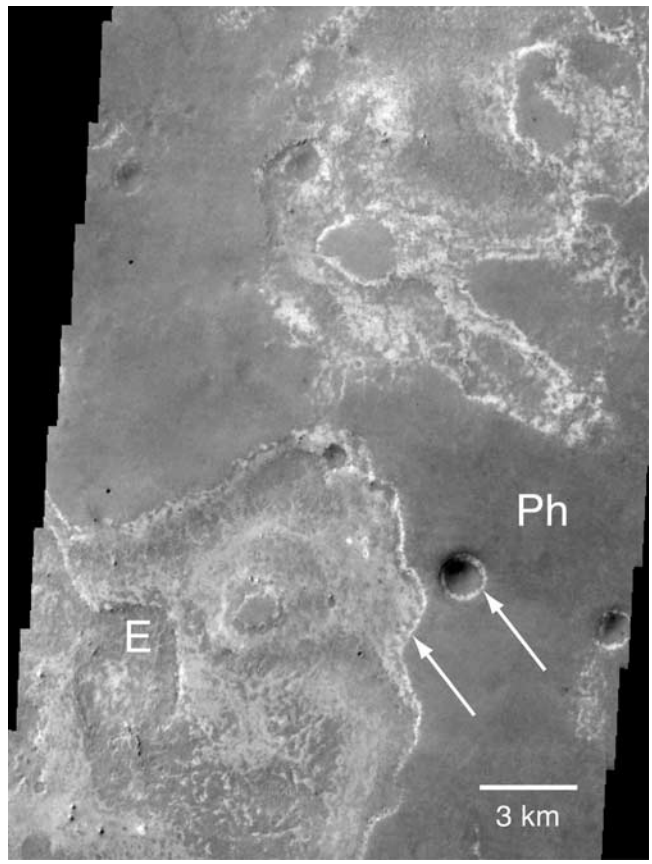

Figure 7. The regional context of a relatively bright layer immediately below the hematite-bearing upper layer of Ph as seen at 36-m resolution by the THEMIS visible camera. This unit is suggested to be the same unit as seen ~300 km to the southwest within the MER-B landing ellipse (Figure 6). This layer is exposed within an inner crater wall and at the margin of the Ph unit (arrows). The etched unit (E) occurs in the lower left corner of this image, several hundred meters below the bright unit. Occurrences of this bright layer occur throughout Ph; this example is in the northeast region of Ph, near rise R. This portion of THEMIS visible image (V03570003) is centered at 0.45°N, 358.6°E.

We suggest that this distinctive unit extends over large portions of the Ph unit, possibly being a single "marker" bed that occurs beneath the overlying hematite unit throughout Ph and formed under similar conditions over a relatively short period of time.

[18] Three subunits of Ph can be identified laterally on the basis of minor differences in their relative thermal inertias derived from the nighttime THEMIS images (Figure 2). Ph-a is a relatively cold (~185 K at a local time of 3.1 H, L_s ~ 340°) unit with a relatively low thermal inertia of ~150, corresponding to an average particle size for uniform, unconsolidated grains of ~40 μm [*Presley and Christensen*, 1997]. This subunit covers over half of Ph, including the western portion of the MER landing ellipse. Ph-b is an intermediate inertia unit with relatively uniform nighttime temperatures of 189–190 K (3.1 H, 336° L_s), corresponding to an average particle size of ~125 μm, that covers ~30% of Ph. This unit occurs in the eastern portion of the landing ellipse. Finally, subunit Ph-c is thermally heterogeneous at spatial scales of ~0.3 to 1 km with temperature variations of 187–195 K covering ~20% of Ph but not exposed within the landing ellipse. These temperatures correspond to thermal inertias of ~200–300, respectively, which correspond to average particle sizes of ~125–750 μm.

[19] In summary, hematite-rich material occurs as a disaggregated surface veneer of an in-place geologic unit.

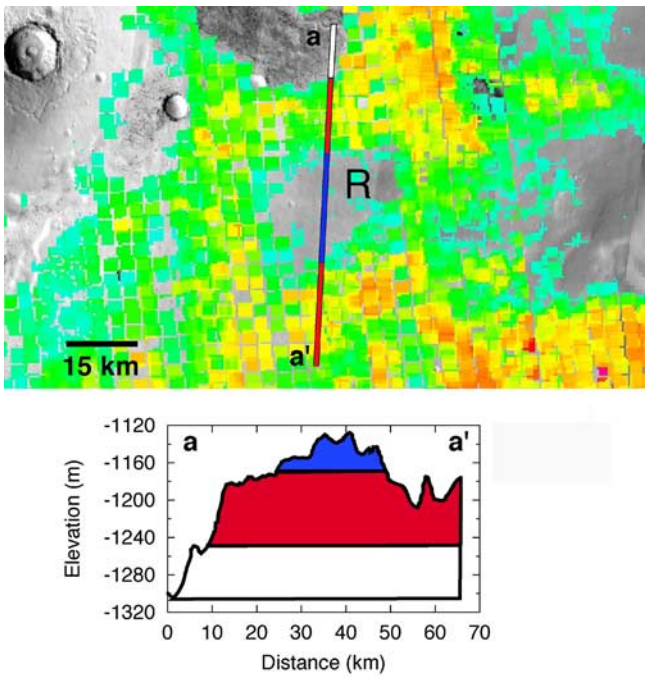

Figure 8a. The hematite-free unit (Pu) at rise R. The hematite abundance derived from TES data is superimposed on a mosaic of THEMIS daytime IR images. The hematite detection threshold is the same as in Figure 3. A topographic profile (a-a′) derived from MOLA gridded data shows that the hematite-free unit (Pu), indicated by the blue bar on the image and the blue layer in the topographic profile, is stratigraphically above unit Ph. The distribution of the hematite-free unit is indicated by the red bar and red layer; the location of the hematite-free unit below Ph is indicated by the white bar and white layer.

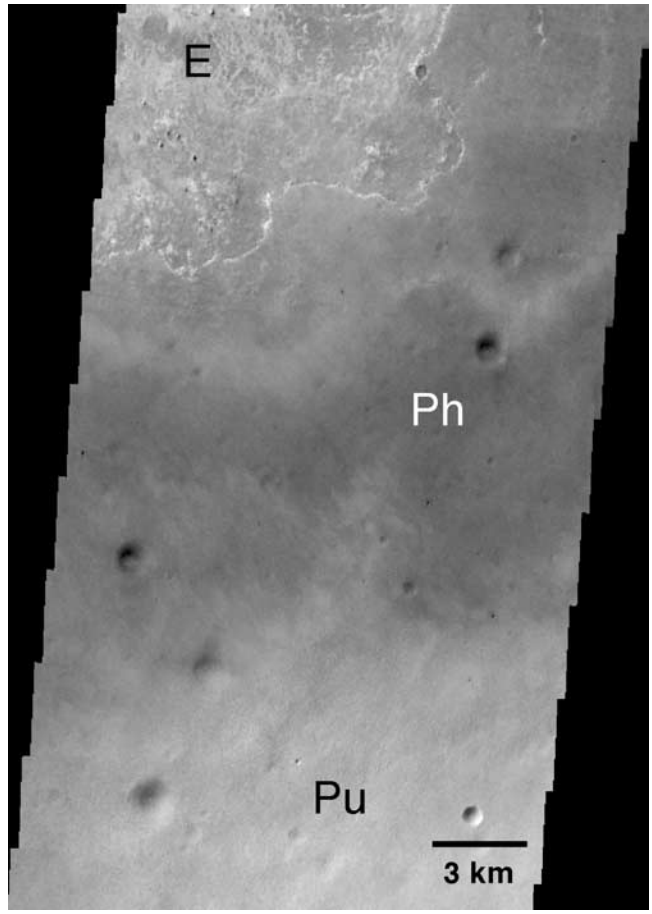

Figure 8b. The contact between the hematite-bearing unit Ph and the overlying hematite-free unit Pu at rise R. The hematite-free etched (E) unit can also be seen in the upper left portion of the image at location "a" in Figure 8a, where the overlying Ph unit has been removed by erosion. THEMIS VIS image V03570003 centered at 0.17°N, 358.5°E. Image resolution is 36 m per pixel.

Hematite is not transported in detectable abundance beyond the margin of this unit. The uppermost surface of Ph has a lower thermal inertia than the underlying etched unit E, and subunits with higher inertia occur within Ph. A thin, relatively bright layer in the vicinity of the MER-B ellipse is proposed to be a layer within Ph that lies just below the hematite-bearing material. A layer of similar thickness and appearance is exposed in Ph ~300 km away, suggesting that this unit may be common beneath the hematite unit and that it and the hematite unit may be genetically related.

2.3. Stratigraphic Relationships

[20] A key question to the origin of hematite is its distribution within and above unit Ph. Insights into this question are found in two regions within the boundaries of the main Ph unit that have little or no hematite exposed on the surface. The first is a 25-km-wide rise centered near 358.4°E, −0.2°S (R in Figure 3). The surface of this rise is up to 50 m above the hematite-rich plains (Figure 8a). There is a distinct topographic break in slope associated with the margins of this rise. At the locations of the breaks in slope that define the margins of this rise, there is a sharp decrease

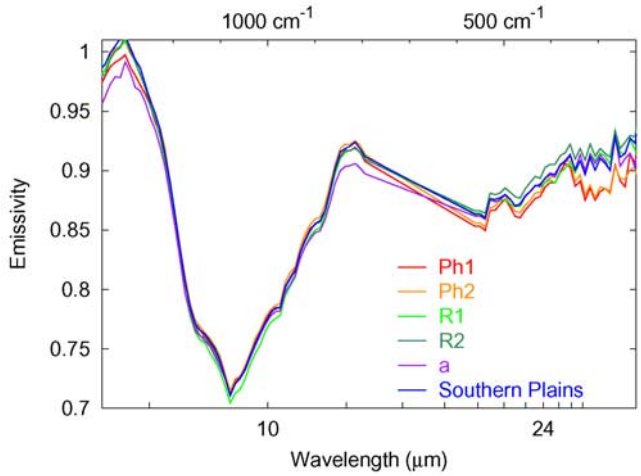

Figure 9a. TES spectra of the hematite-poor surface of rise R compared to the hematite-rich Ph unit. Spectra over the spectral range from 1350 to 350 cm^{-1} are shown from a region of high hematite immediately south of R (Ph1) and a second region ~50 km farther south (Ph2). Spectra from rise R (R1 and R2) are from two consecutive TES observations. Spectra from surfaces that do not have hematite (a and Southern Plains) are shown for reference. The surface of rise R has significantly less hematite than the neighboring Ph surfaces, and the abundance on this surface is comparable to hematite-free plains. All spectra are from a single TES orbit and are averages of all six detectors collected simultaneously, covering an area ~9 by 6 km in size.

in hematite abundance (Figure 8a). Figures 9a and 9b show TES spectra acquired on a single orbit that crosses the boundary between the hematite-rich Ph surface and the rise R. As seen in Figures 9a and 9b, the two hematite absorptions at ~300 and 480 cm^{-1} are readily apparent in the representative spectra from unit Ph at band depths corresponding to abundances of ~15%. The depths of these absorption bands are significantly reduced or absent in the spectra from the rise. This marked decrease in hematite band depth in the material on rise R indicates that this overlying material has significantly less hematite than the material immediately below.

[21] The topography and hematite abundance observations suggest that the material that comprises rise R is a stratigraphic unit (designated Pupper or Pu) that lies immediately above the hematite-bearing unit of Ph. The transition from hematite-rich to hematite-poor materials occurs over a maximum vertical distance of ~20 m (Figure 8a) and may occur at the contact between Ph and Pu.

[22] A THEMIS visible image of this area (Figure 8b) shows that the morphology and crater abundance of Ph and Pu are similar. The contact is gradational, with isolated remnants of the overlying Pu unit occurring away from the main body, indicating that this unit was removed by erosion. The overlying Pu unit appears to lie conformably on the hematite-bearing unit, with no evidence that Ph underwent erosion prior to the deposition of the overlying unit. This relationship suggests that there was no significant gap in time between the deposition of the two units. The gradational character of the contact also indicates that there are no significant differences in the competency of the two units, suggesting that the two units were deposited under similar conditions and processes.

[23] A similar example of an overlying, hematite-poor layer is observed in an eroded, 30-km-wide mesa (Figure 10) centered at 358.5°E, 2.5°N near the northern margin of Ph (M in Figure 3). This unit appears to lie directly on top of the dissected cratered terrain unit at this location, without the intervening etched unit. As discussed by *Arvidson et al.* [2003], the etched unit lies unconformably on top of unit DCT throughout Meridiani. It appears that in some locations, such as a mesa M, unit Ph also lies unconformably on top of the DCT.

[24] Hematite abundance varies across mesa M, decreasing significantly on the eastern and western margins (Figure 3). These hematite-poor surfaces rise ~20–30 m above Ph. The Ph surface exposed in the center of the mesa is smoother than the hematite-poor surfaces, which have a distinctive erosional texture of subtle pits at 100-m scales and resemble subtle surface textures at rise R. As seen at R, the overlying surface at M appears to lie conformably on top of the hematite unit, with no evidence for a significant change in depositional environment and no evidence for a discontinuity in time between the deposition of the two units.

[25] The low abundance of hematite on the overlying layer provides strong evidence that hematite is not a lag deposit eroded from the overlying layers because it should be present in significant amounts on the surface of these overlying layers as well if it was contained within them. Therefore it appears that the hematite originates from the layer where it is currently observed.

[26] The eastern slope of the mesa at M is 3–5 km wide and exposes the entire Ph unit down to the dissected cratered terrain on which it appears to lie (Figure 10). This slope is wide enough to be resolved by TES yet has no detectable hematite. The lack of hematite on this slope suggests that the lower layers of Ph may not contain hematite. The southwest margin of Ph near 352.8°E, 3.2°S

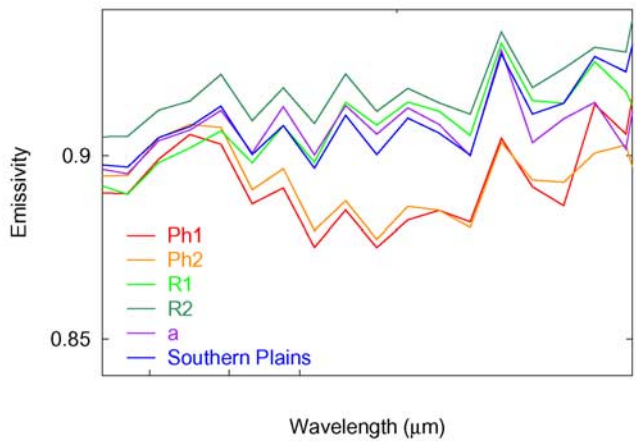

Figure 9b. TES spectra of the hematite-poor surface of rise R compared to the hematite-rich Ph unit over the spectral range 400 to 220 cm^{-1}. This spectral region contains the strong hematite absorption band observed by TES.

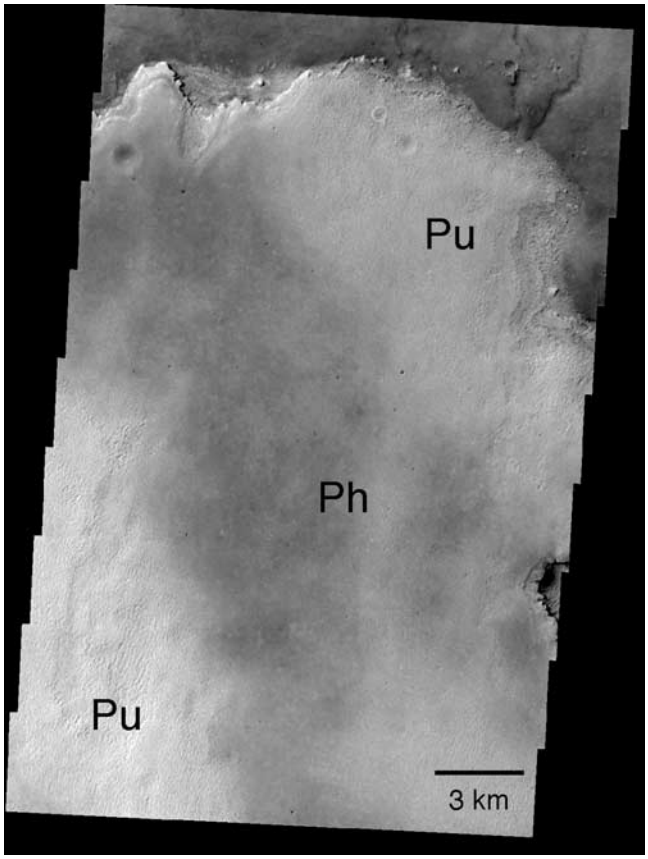

Figure 10. The surface of mesa M. Outcrops of the hematite-free unit (Pu) occur on the western and eastern margins of this mesa. The central portion is topographically lower than the margins and has hematite exposed on the surface. The older dissected cratered terrain on which the Ph and Pu units were unconformably deposited can be seen in the upper right portion of this image. THEMIS visible image V03280003, centered at 2.7°N, 358.4°E. Image resolution is 18 m per pixel.

is also a broad gentle slope on which the entire thickness of Ph again is exposed. The TES hematite abundance decreases down this slope, suggesting that hematite may occur only in the topmost layer.

[27] The nighttime temperatures of M on the eastern and western hematite-free surfaces are 6–12 K colder than the central hematite-rich surface (Figure 2). These temperature differences indicate that the hematite-rich surface, while typically lower thermal inertia than the surrounding etched and dissected cratered terrains, has a higher inertia than the material stratigraphically above. This observation is consistent with the nearly complete removal of a slightly less competent overlying layer down to current surface of Ph.

[28] The southern margin of the hematite unit appears to embay the highstanding terrain to the south (Figure 11), as originally noted by *Edgett and Parker* [1997] and discussed by subsequent authors [*Christensen et al.*, 2000b; *Hynek et al.*, 2002]. This relationship suggests that the hematite-bearing unit was originally deposited in a dense, gravity-controlled fluid, rather than as a dispersed, air fall layer.

[29] There are only three occurrences of the hematite-bearing unit exposed south of the main Ph deposit (Figure 3). All occur within craters that are 20–40 km in diameter and are within 50 km of the southern margin. All of these occurrences appear to be eroded remnants of once-larger deposits. The elevations of the upper surfaces of these outliers are ~300–700 m below the average level of the top of the main hematite-bearing unit and ~200–700 m below their respective crater rims. No hematite is observed on the intracrater plains of the ancient cratered terrain south of Ph, which vary in elevation from several hundred meters below to several hundred meters above the hematite-bearing unit. This lack of any detectable hematite on the plains units indicates that either hematite material was not deposited as a widely distributed air fall or this material has been completely removed from the plains surfaces.

[30] Finally, the morphologic and thermophysical properties of the Etched and Ph units are different, as reflected in the fact that these materials have been mapped as distinct units on the basis of these properties [*Hynek et al.*, 2002; *Arvidson et al.*, 2003]. Figures 12a and 12b show two THEMIS VIS images and a mosaic of THEMIS IR images that illustrate the significant differences in the properties of these units. Possible causes are (1) differences in density and porosity between igneous and clastic sedimentary materials or among igneous materials; (2) variations in particle size and sorting among different sedimentary deposits; and (3) variations in the degree of lithification or cementation among initially similar clastic or pyroclastic materials [*Christensen et al.*, 2003a]. Whatever the cause, the observed differences in morphologic and thermophysical characteristics between the Etched and Ph units imply temporal changes in the processes or environments that formed them [*Christensen et al.*, 2003a].

[31] In summary, the hematite-bearing unit appears to be a relatively thin upper unit in Ph, with higher-inertia material immediately below. The occurrence of hematite-free units directly above the hematite unit provides strong evidence that whatever mechanism formed the hematite was sharply confined vertically and/or in time. The hematite unit appears to embay preexisting channels, occurs as outliers within closed crater basins, has significantly different properties from the Etched unit below it, and is absent from the

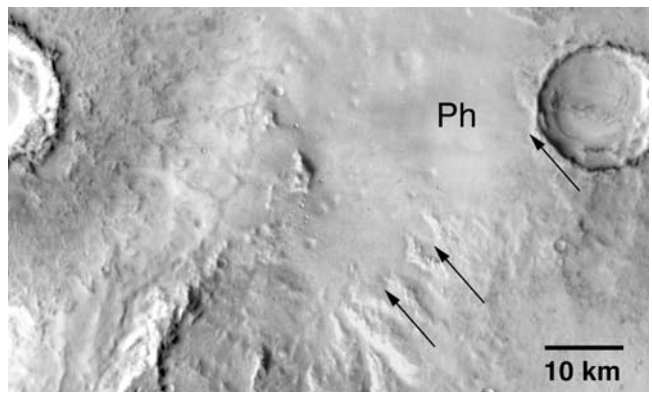

Figure 11. Embayment relationships on the southern margin of the hematite-bearing unit Ph. The location of the embayment margin is indicated by arrows. This daytime infrared image is an enlarged and image-enhanced segment of Figure 1. Image resolution is 100 m per pixel.

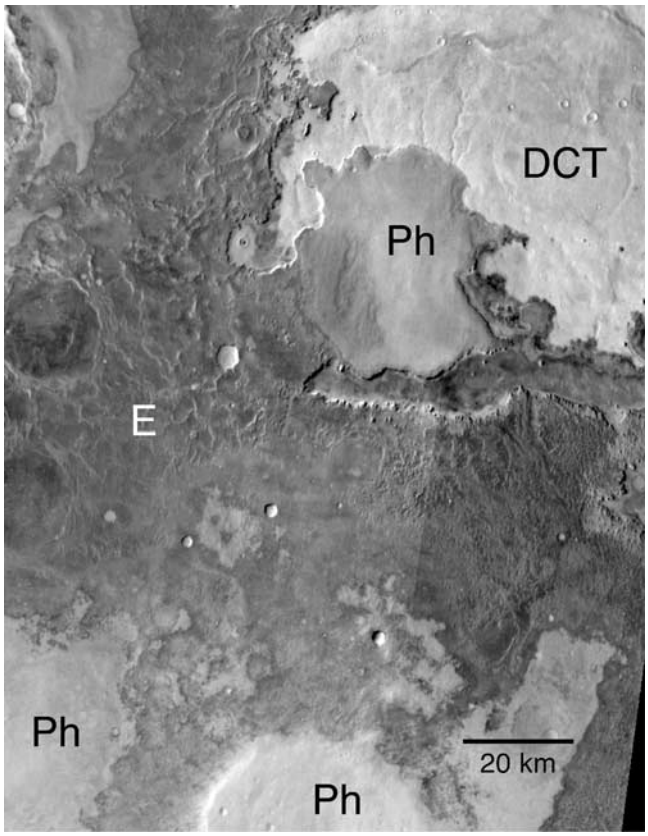

Figure 12a. Comparison of surface morphology of the hematite-bearing unit (Ph), the lower etched unit (E), and the dissected cratered terrain (DCT). The Ph unit in the upper right portion of the figure is the mesa (M) in Figures 1, 2, 3, and 10. It is characterized by a smooth surface with layers exposed in eroded slopes. The etched unit appears to be eroded into a series of ridges and small mesas. The Ph unit appears to have been deposited unconformably on the etched unit. The cratered terrain is the oldest surface, and both the Ph and E units were deposited unconformably on this unit. A series of channels were eroded into the DCT unit prior to the deposition of Ph. These channels slope southward toward the current location of the Ph unit in mesa M. The semicircular occurrence of Ph in the lower center of the figure is a portion of a circular deposit interpreted to have been formed within the walls of a crater basin that has since been completely removed. This figure is an enlarged portion of the daytime infrared mosaic shown in Figure 1. Image resolution is 100 m per pixel.

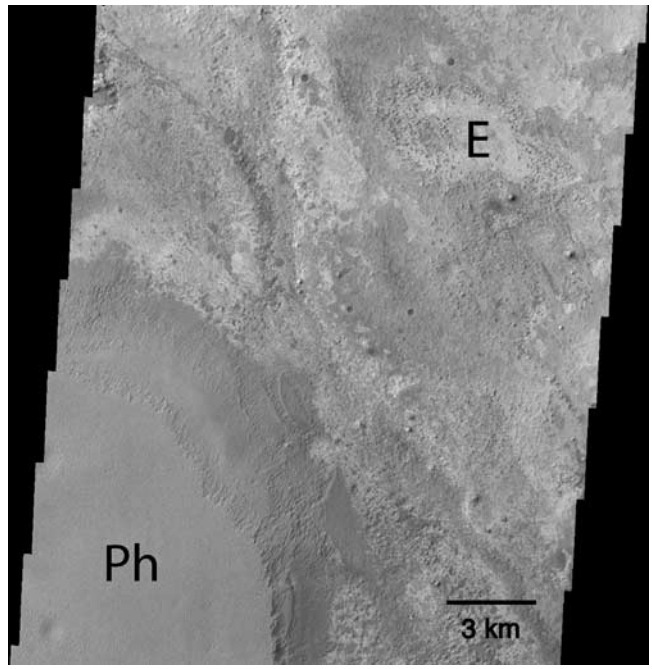

Figure 12b. Comparison of the textures of the etched unit E and the hematite-bearing Ph unit. This THEMIS visible image shows the contact of Ph with the underlying etched unit E. This portion of THEMIS image V03520003 covers an area 18 km × 20 km in size, centered near 1.2°N, 0.5°E with a resolution of 18 m per pixel.

surrounding plains, suggesting that it may have been deposited in a dense fluid, rather than as a dispersed air fall.

2.4. Topographic Relationships

[32] A series of eight topographic profiles taken across Ph are shown in Figures 13a and 13b. Along the length of the southern margin of Ph the contact is a local topographic minimum, with the cratered highlands rising several hundred meters to the south and the hematite unit rising 100–400 m to the north, typically with a convex upward slope (Figures 13a and 13b). The elevation of the hematite unit above the contact increases from a low of ~100 m in the east to ~150–200 m in the central region to a maximum of ~400 m in the southwest.

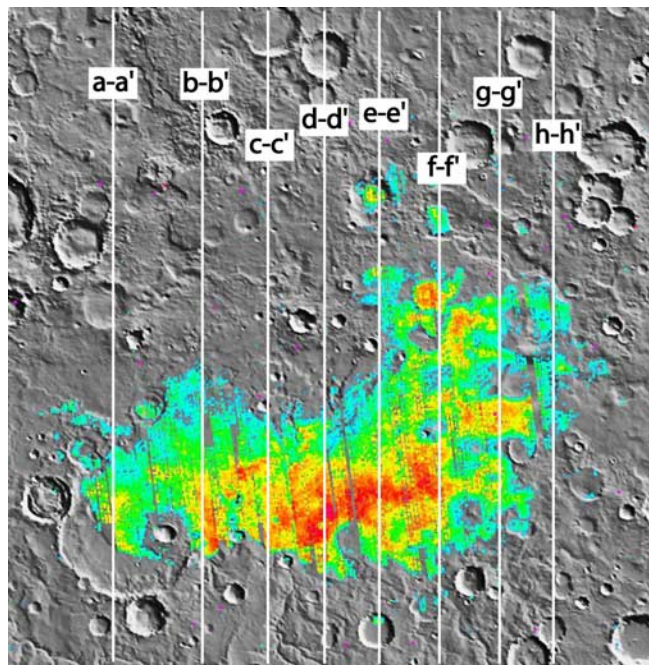

Figure 13a. The location of topographic profiles across Meridiani Planum. The positions of eight profiles are shown on a map of hematite abundance derived from TES data and a MOLA-derived shaded relief image. Hematite abundances vary from ~5% (blue) to ~20% (red).

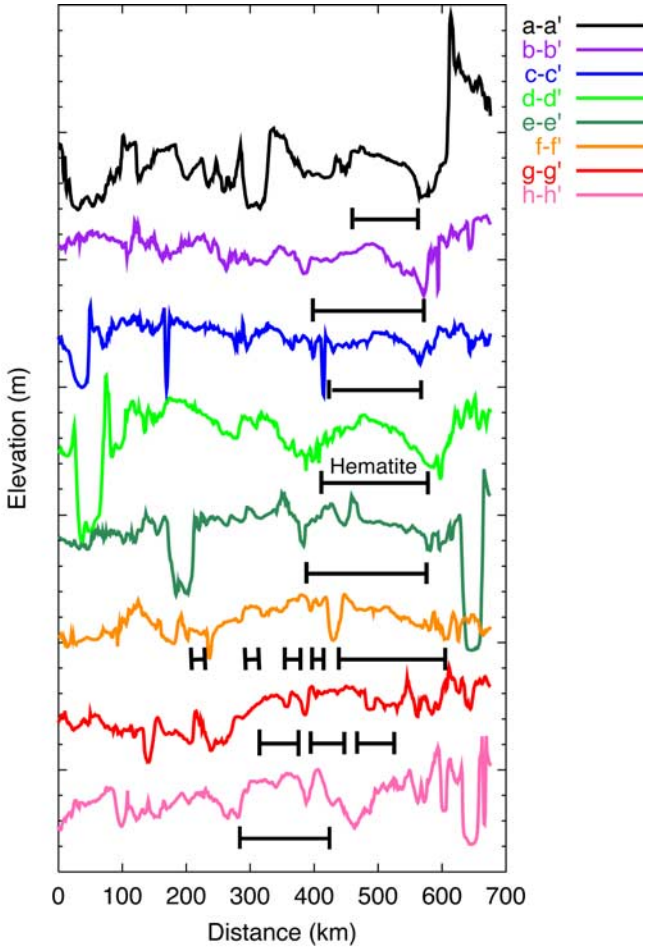

Figure 13b. Topographic profiles for the locations shown in Figure 13a. The location of the hematite-bearing unit (Ph) of the Meridiani Formation is shown by horizontal bars on each profile. The vertical elevation scale is 200 m per tic; profiles have been vertically offset for clarity. Unit Ph is in a topographic trough in profiles a-a′ through e-e′ and is bounded by a topographic rise to the south on all profiles except f-f′. Unit Ph is 50–150 m higher than the bounding units to the north in the three eastern profiles, f-f′, g-g′, and h-h′.

This increase in apparent unit thickness toward the west may be due to deposition within a preexisting 140-km-diameter crater (Figures 13a and 13b). Along the western margin, Ph rises ~250 m from the nearby plains.

[33] Along its northern and eastern boundary, Ph is in contact with several different units that are interpreted to predate Ph [*Christensen et al.*, 2001; *Hynek et al.*, 2002; *Arvidson et al.*, 2003; *Newsom et al.*, 2003]. There is typically less than 50 m of elevation change across this contact, and in the central and western sections the bounding units are 50–100 m higher than Ph (Figures 13a and 13b; profiles a-a′ through f-f′). North of the contact the bounding Ph and E units typically vary in elevation by only ±50 m over a distance up to 250 km from the hematite unit (Figures 13a and 13b).

[34] The northern, eastern, and western margins of Ph are discontinuous with numerous outliers up to 60 km in size and separated by up to 200 km from the main deposit (Figure 3). In many cases these outliers have exposed layers and margins interpreted to have receded by erosion [*Arvidson et al.*, 2003; *Newsom et al.*, 2003]. Along the central portion of the northern boundary, these outliers may be eroded remnants of a once continuous layer [*Christensen et al.*, 2000b, 2001; *Hynek et al.*, 2002; *Arvidson et al.*, 2003; *Newsom et al.*, 2003]. However, the most distant outliers occur within large (>30- to 45-km-diameter) craters or as circular or quasi-circular deposits surrounded by circular troughs, suggesting that they were also deposited inside preexisting craters whose rims have since been removed by erosion. The lack of hematite material exposed on the plains between the main Ph unit and the occurrence of these distant outliers may indicate that these outliers were deposited within isolated closed crater basins and that the hematite-bearing unit was not deposited as a continuous layer over the entire surface.

[35] Nine craters ranging in diameter from 2 to 25 km within Ph have either excavated through or deposited ejecta on Ph, resulting in low hematite abundance at TES resolution (Figure 3). These craters are centered, from east to west, at 353.8°E, −3.0°S (22-km diameter), 354.8°E, −2.7°S (10-km diameter), 355.6°E, −2.7°S (7-km diameter), 356.4°E, −2.8°S (6-km diameter), 356.9°E, −3.3°S (2-km diameter), 357.6°E, −2.5°S (5-km diameter), 357.8°E; −1.2°S (7-km diameter), 358.3°, −1.2°S (11-km diameter), and 358.3°E, −2.3°S (9-km diameter). Thermally distinct crater ejecta rays from many of these craters are present on Ph (Figure 2), indicating that they postdate the unit's formation. The lack of detectable hematite on the ejecta from these craters, including one only ~2 km in diameter, suggests that the hematite-bearing layer is significantly thinner than the depth to which these craters excavated (<~0.2 km [*Melosh*, 1989]).

[36] A 22-km-diameter impact crater located at 354.9°E, −2.3°S has hematite-bearing material draping the NW wall and onto the floor (Figure 3; C). The upper surface of the hematite unit drops ~180 m in 3.5 km (3° slope) down the NW inner crater wall and then an additional 200 m over 11 km (1° slope) across the crater floor. In the SE region of the crater the floor materials drop an additional 120 m in 3.5 km (2° slope). Truncated rock layers are exposed along this slope, indicating that this is an erosional surface. This lowest region of the crater does not have hematite exposed at the surface (Figure 3), suggesting that the hematite-bearing unit has been completely removed by erosion in this area. Unit Ph clearly drapes the preexisting topography at this location and was deposited either subaerially or subaqueously onto an older landscape. No distinctive morphologies are observed to distinguish these two modes, and the slopes of these surfaces are low enough (1°–3°) to permit either process to have occurred.

2.5. Morphology

[37] The surface of Ph has a distinct character of smooth plains and subdued crater morphologies (Figure 14). It has been suggested that this material may be an eroded volcanic ash deposit on the basis of its layered, friable surface character [*Hynek et al.*, 2002, 2003]. Extensive deposits of eroded friable material have been mapped throughout the equatorial region, such as within the Medusae Fossae Formation, and many of these have been proposed to be ash deposits [*Hynek et al.*, 2003]. In general, however, the

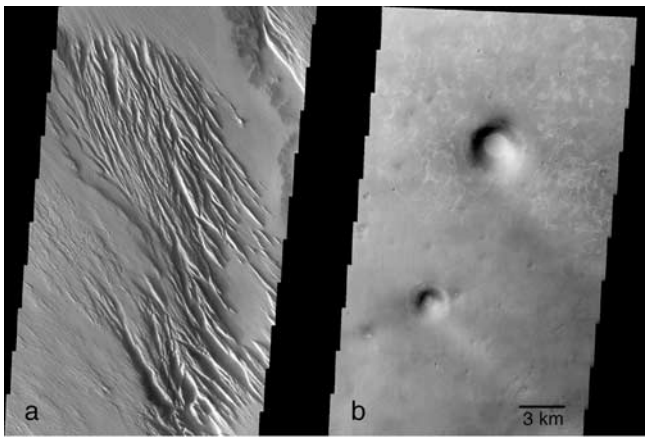

Figure 14. Comparison of the surfaces of proposed ash deposits of (a) the Medusa Fossae unit and (b) the Meridiani hematite-bearing unit Ph. The Meridiani units have a flat-lying surface with unique, subdued crater morphologies and no evidence of yardang-style erosion. The Medusae Fossae materials are characterized by erosion into yardangs. Each image is a portion of a THEMIS visible image with an image resolution of 18 m per pixel. Medusae Fossae image is from V06560001, centered at 5.1°S, 200.3°E; Meridiani image is from V01836001, centered at 1.9°S, 354.3°E.

surface of Ph does not appear to erode like putative ash deposits (Figure 14). *Hynek et al.* [2003] suggest that the differences may be due to secondary alteration that produced the observed mineralogy. Alternatively, the Meridiani unit may not be volcanic ash and was formed by a different process than the deposition of air fall ash.

[38] Unit Ph is also strikingly different from the underlying units E and DCT (Figure 12). It erodes in a significantly different manner, lacks the connected series of ridges found in unit E [*Arvidson et al.*, 2003], shows clear evidence of layering that is unlike units E and DCT, has a lower thermal inertia, appears to be deposited on both E and DCT, and contains hematite.

[39] Both the Ph and E units were deposited unconformably on the older cratered terrain [*Hynek et al.*, 2002; *Arvidson et al.*, 2003]. A series of channels were eroded into the DCT unit prior to the deposition of Ph [*Newsom et al.*, 2003]. These channels appear to have flowed southward toward the current location of the Ph unit in mesa M, suggesting the possible flow of water into a local basin where this mesa formed.

[40] We suggest that while unit Ph lies atop units E and DCT, its physical and compositional properties point to a significantly different environment of deposition. *Arvidson et al.* [2003] suggested that Ph and E were deposited unconformably on top of the older cratered terrains. We concur with this interpretation, but suggest that Ph was formed under different conditions and processes than the underlying E units.

3. Discussion

[41] The formation modes for the gray crystalline hematite detected by TES were grouped into two classes by *Christensen et al.* [2000b, 2001]: (1) chemical precipitation and (2) thermal oxidation of magnetite-rich volcanic materials. The chemical precipitation models they proposed were (1a) low-temperature precipitation of Fe oxides/oxyhydroxides from standing, oxygenated, Fe-rich water, followed by subsequent alteration to crystalline hematite, (1b) low-temperature leaching of iron-bearing silicates and other materials to leave a Fe-rich residue (laterite-style weathering) which is subsequently altered to crystalline hematite, (1c) precipitation of Fe oxides or crystalline hematite from Fe-rich circulating fluids of hydrothermal or other origin, and (1d) formation of crystalline hematitic surface coatings during weathering. Models 1a and 1b require an alteration process (e.g., burial metamorphism) to convert Fe oxide/hydroxide assemblages (e.g., goethite, red hematite, ferrihydrite, and siderite) to crystalline gray hematite.

[42] On the basis of the analysis of TES, MOC, and MOLA data, *Christensen et al.* [2001] could not exclude any of these models but favored the two models in which the deposits of crystalline gray hematite were formed either by chemical precipitation of hematite (or a goethite precursor [*Glotch et al.*, 2004]) from Fe-rich aqueous fluids under ambient (model 1a) or by hydrothermal processes (model 1c). Subsequent analysis by *Lane et al.* [2002] proposed the precipitation of Fe oxides that were metamorphosed by burial to platy hematite and subsequently exposed by erosion. *Hynek et al.* [2002] favored precipitation from Fe-rich circulating fluids (model 1c) or thermal oxidation of volcanic ash during eruption (model 2). *Newsom et al.* [2003] suggest, but do not distinguish between, precipitation from standing water, precipitation as coatings from groundwater, or oxidation of preexisting minerals. *Catling and Moore* [2003] favored Fe-rich hydrothermal fluids as the emplacement mechanism for the formation of hematite at Aram Chaos on the basis of both geochemical and geomorphologic evidence.

[43] The close correlation of hematite-bearing material with specific rock units argues against an external process of surface coating (model 1d). It is possible that a reaction occurred between the atmosphere or groundwater and material in a specific rock unit, but in this case the process is best characterized by one of the models by which this material was originally deposited. The lack of any evidence for extensive surface runoff argues against a surface chemical leaching process (model 1b). Each of the remaining three models will be discussed in light of the observations presented above, with an emphasis on the major points for, and against, each mechanism.

3.1. Oxidation of Magnetite-Rich Ash

[44] The oxidation of magnetite-rich ash combines the hematite precursor (magnetite) and the alteration mechanism (heat of eruption) into a single process. Ash provides an easily erodible material, and multiple eruption events can produce the observed variations in layer competency [*Hynek et al.*, 2002]. However, high-temperature oxidation of magnetite does not produce spectra that match the TES observations [*Glotch et al.*, 2004]. In addition, the occurrence of hematite in terrestrial volcanic deposits, such as El Laco, Chile, or Kiirunavaara, Sweden, may be derived from late-stage hydrothermal activity, rather than in-air oxidation [*Catling and Moore*, 2003; *Bookstrom*, 1995; *Parak*, 1975].

These types of deposits are also dominated by magnetite, yet this mineral is not detected in the TES observations of hematite-rich surfaces [*Catling and Moore*, 2003]. An air fall deposit can account for the draping of topography, such as at crater C (Figure 3). The apparent thickness of material in this crater is comparable to that outside, consistent with uniform deposition from above. However, the embayment relationships and the lack of hematite-rich material on the plains to the south argue against a dispersed air fall deposit. The truncation of layers in embayment contacts instead suggests a dense surface flow or subaqueous deposition, and the lack of material on the plains would require that any deposited ash has been completely removed. The uniformity of hematite abundance across the deposit would require a massive eruption of ash of uniform composition that differed from the layer deposited immediately above, and possibly below (e.g., at R and M), and which differs in composition and morphology from other possible ash deposits on Mars. Finally, the coarse-grained basaltic composition of the primary component of Ph is not consistent with a fine-grained, presumably glassy, ash deposit.

3.2. Hydrothermal Alteration of Preexisting Rock Units

[45] Hydrothermal fluids can dissolve Fe from preexisting rocks, which can then be precipitated as hematite or as Fe oxyhydroxides that are subsequently dehydroxylated to hematite. Both of these mechanisms produce good matches to the TES spectra [*Glotch et al.*, 2004]. However, the transition from hematite-rich to hematite-poor material at the contact between Ph and Pu occurs over a vertical distance of only several meters. The presence of unaltered layers immediately above the Ph unit would require that the proposed alteration did not extend into these layers, despite occurring over an area more than 150,000 km^2 in size. This sharp vertical boundary between a proposed altered unit (Ph) and one directly above that has little or no hematite (Pu) is not consistent with a regional hydrothermal process. It is possible that the hematite-poor unit was deposited after the alteration occurred. However, there is no evidence for this in an unconformity or significant change in unit characteristics between Ph and Pu. Finally, the lack of a systematic lateral variation in hematite abundance across Ph suggests that there was no significant variation in the degree of alteration across this large area and that there was no apparent center or focus of this alteration, again inconsistent with regional alteration.

[46] If hydrothermal alteration did occur, then several sources of the altering fluids can be considered. The fluids could have originated from a regional source below Ph, but the presence of unaltered basaltic material below Ph (unit E) makes this source unlikely. The fluids could have moved laterally through Ph, confined at the base by an impermeable layer that could have been the high-inertia subunit of Ph or the Etched unit. However, a significant difficulty with this model is the presence of hematite within distant, preexisting craters in different terrains and at significantly different elevations. It is unlikely that a single impermeable layer would exist both inside and outside the craters, that fluids would migrate through the disrupted crater walls, or that fluids would migrate through Ph only in these different locales. The fluids could have come from above, such as from the melting of an overlying snow or ice deposit. These waters would melt and move downward, be heated by some thermal source, dissolve iron, and then precipitate hematite or its precursor. However, with this model it is again difficult to account for the sharp transition from hematite-poor to hematite-rich materials within several meters of elevation as seen at R and M.

3.3. Deposition of Hematite or Precursor Fe Oxides or Oxyhydroxides in Water

[47] The deposition of hematite or precursor Fe oxide/hydroxides in water can resolve many of the difficulties discussed above. The formation of goethite, followed by dehydroxylation to hematite, provides the best match to the observed TES spectra [*Glotch et al.*, 2004]. Deposition from standing water could account for the hematite occurring in a thin, widespread, uniform, friable unit, with deposition of hematite, or precursor Fe oxide/hydroxides [*Glotch et al.*, 2003], occurring as the temperature, Ph, or Eh of the water changed with time. In this mechanism the sharp boundaries at the top, and possibly bottom, of the hematite layer were produced by changes in depositional environment, rather than requiring changes in hydrothermal alteration over meter-scale vertical distances. Deposition of a precursor material in standing water would account for the large lateral, but small vertical, extent of the hematite layer. The currently exposed surface of Meridiani varies in elevation by $\sim$100 m and in hematite abundance from $\sim$5 to 20%. The variations may reflect local erosion, with hematite varying in abundance as it is removed or slightly concentrated as a surface lag as the hematite-bearing layer is deflated. The similarity in the character of the hematite-bearing unit in Ph with Pu could be explained by their being deposited under similar environments that differed only in the precipitation of relatively minor amounts of Fe oxides. Deposition of Fe oxide precursor was proposed by *Lane et al.* [2002], followed by burial metamorphism and erosion to expose the material. Recent laboratory measurements indicate that burial metamorphism is not required to reproduce the hematite spectral character observed by TES [*Glotch et al.*, 2004].

[48] *Burns* [1993] initially suggested that banded iron formation (BIF) may have occurred on Mars on the basis of the likely occurrence of iron-rich fluids. This possibility has been explored for a range of chemical, photostimulated, and biologic oxidation to produce precursor Fe oxides, followed by low-grade thermal transition to hematite (see review by *Catling and Moore* [2003]). On the Earth, precipitation of Fe oxyhydroxides from iron-rich water followed by low-temperature, low-pressure dehydroxylation has been proposed for the formation of hematite in banded iron formations [*Krapez et al.*, 2003]. In a model developed for the Hamersley Province of Australia the precursor sediments to BIF are interpreted to have been hydrothermal muds composed of iron-rich oxyhydroxides, smectite, and siderite that were deposited on the flanks of submarine volcanoes and transported by density currents [*Krapez et al.*, 2003]. Hematite spheroids in these sediments closely resemble those found in modern Red Sea iron oxide deposits [*Butuzova et al.*, 1990] and are likely diagenetic transformations of iron oxyhydroxide muds [*Krapez et al.*, 2003; *Bischoff*, 1969a, 1969b]. Alternating Fe oxide and

silica layers in the Hamersley BIF are compacted density current laminations, with the chert being diagenetic and developed during burial [*Krapez et al.*, 2003]. The conditions on Mars may have been sufficiently different from the terrestrial examples for silica not to have been precipitated, resulting in a sequence consisting only of Fe oxides [e.g., *Fernández-Remolar et al.*, 2004].

[49] An aqueous origin for the hematite deposits in Meridiani has been proposed on the basis of analogy to the Rio Tinto iron formations of Spain [*Fernández-Remolar et al.*, 2004]. This extreme acidic environment has water that is rich in ferric iron and sulfate that produces sediments dominated by ferric oxyhydroxides and sulfate minerals, with no silica phases [*Fernández-Remolar et al.*, 2004]. These iron formations suggest that the iron phase has changed over time from iron oxyhydroxides and sulfates to hematite-goethite-dominated associations through dehydroxylation and desulfation [*Fernández-Remolar et al.*, 2004]. This mechanism would account for the lack of other minerals detected by the TES in Meridiani and accounts for the development of coarse-grained crystalline hematite [*Fernández-Remolar et al.*, 2004]. This model accounts for the lack of silica in Meridiani by the occurrence of a standing body of water fed by underground iron-rich sources whose chemistry and thermodynamics favored precipitation of iron-bearing phases but not silica [*Fernández-Remolar et al.*, 2004].

[50] To form hematite from standing water on Mars, both a source of oxidation and the necessary conditions for dehydroxilation to hematite are required [*Catling and Moore*, 2003]. Fine-grained goethite is thermodynamically unstable relative to hematite plus water [*Berner*, 1969; *Langmuir*, 1971]. Laboratory studies have shown that dehydroxilation to hematite can occur within a few weeks in water at temperatures between 70° and 130°C [*Tunell and Posnjak*, 1931; *Catling and Moore*, 2003; *Johnston and Lewis*, 1983; *Vorobyeva and Melnik*, 1977; *Schmalz*, 1959; *Wefers*, 1966]. Thermodynamic data of Diakonov et al. were used by *Catling and Moore* [2003] to construct a phase diagram for goethite-hematite in which the transition to hematite occurs at 100°C. Thermodynamic calculations by *Berner* [1969], however, indicate that the maximum temperature at which fine-grained goethite is stable relative to hematite is ~40°C. Natural occurrences where the temperatures are constrained by oxygen isotope evidence suggest that the temperatures of these natural systems are >100°C [*Catling and Moore*, 2003]. However, the transformation from iron oxyhydroxide phases to dehydroxylated hematite in the Rio Tinto, Spain, system has been suggested by *Fernández-Remolar et al.* [2004] to imply that hematite may be formed by dehydration pathways in shallow diagenesis and lower-temperature conditions rather than deep burial. In summary, the available thermodynamic, laboratory, and field data suggest that the transition from goethite to hematite in saturated conditions can occur at temperatures between 40° and 100°C. These temperatures imply modest heating and relatively low-temperature diagenesis. The source of this heat may have been burial to depths of several kilometers [*Catling and Moore*, 2003] or may have been produced by subsurface magmatic heat. Evidence for significant subsurface heating in Meridiani Planum is seen in the basaltic volcanic plains that comprise the units below Ph [*Christensen et al.*, 2000b; *Hynek et al.*, 2002; *Arvidson et al.*, 2003] and the melting of vast amounts of subsurface ice in equatorial chaotic terrains and catastrophic outflow channels.

[51] An obvious argument against precipitation from a standing body of water is the present lack of a confining topographic rise on the northern margin of Ph. *Hynek et al.* [2002] and *Arvidson et al.* [2003] have suggested that Ph is part of thick set of units (P1–P3, Etched) extending over hundreds of kilometers to the north that were deposited on a regional slope and have since been extensively eroded. *Phillips et al.* [2001] argued that this slope formed during the Noachian prior to the deposition of Ph on the basis of the presence of preexisting channels that preferentially flowed down this regional slope. Crater counts have confirmed that the hematite unit is Noachian in age [*Hynek and Phillips*, 2001; *Hynek et al.*, 2002; *Lane et al.*, 2003] and formed near the time that this slope was developing. If all of the units in Meridiani were deposited in water, then the basin boundary would also have to be 500–600 km to the north, where the current topography is ~600 m below the hematite layer [*Hynek et al.*, 2002]. However, the hematite-bearing unit differs significantly from the etched unit E in morphology, thermal inertia, erosional style, heterogeneity, and hematite abundance, suggesting that these two units were deposited in significantly different environments.

[52] An alternative scenario is suggested here, in which unit Ph, but not unit E, was deposited within a series of local, water-filled basins. *Arvidson et al.* [2003] interpreted the Etched unit to be lava flows subjected to extension that fractured the flows into polygons, followed by emplacement of dikes and flows and further extension to form horst-graben patterns. They interpret units P and Ph to be a subsequent stage of the volcaniclastic activity that blanketed the Etched unit. The model proposed here suggests a similar set of events, except that Ph was deposited in water, rather than as a volcaniclastic layer. In both models the materials that make up the Etched and Ph units are significantly different. We argue that the deposition of Ph in water or as volcaniclastic material cannot be distinguished on the basis of stratigraphy. What is important to the standing water model is that units Ph and Etched were deposited in different environments. The apparent deposition of Ph directly on unit DCT (Figure 10) indicates that Ph was deposited in regions where unit E was not, providing additional evidence that Ph was deposited in a different manner than unit E. We propose that units Ph and E were deposited under different conditions and that only the relatively thin Ph unit, not the entire sequence of Etched units, was deposited in water. In this case, only a basin of the size necessary to contain the Ph unit needs to be considered.

[53] In the standing water model proposed here the coarse-grained basalt that makes up the majority of the material of Ph was deposited as clastic sediments within these bodies of water. The northern margin of Ph from ~1°S at 356°E and 1°N at 359°E (Figure 3) represents the northernmost extent of the main basin. This local basin may be related to the large impact basin inferred from MOLA data [*Frey*, 2003; *Newsom et al.*, 2003]. Outliers of hematite-rich material to the north, west, and south are proposed to have been deposited within craters that formed

separate closed basins. The deposition of hematite within these separate bodies of water accounts for the lack of hematite observed on the intracrater plains.

[54] Morphologic evidence from MOC and THEMIS imaging has suggested the occurrence of flow and deposition into standing water in closed basins elsewhere on Mars [*Malin and Edgett*, 2003; *Moore et al.*, 2003]. In many locations, Ph lies within a local trough (Figures 13a and 13b), and in places where Ph is higher than its surroundings, this elevation difference is less than 50–100 m (Figures 13a and 13b). If Ph was deposited contemporaneously with regional tilting, then minor tilting of the region, i.e., several hundred meters over several hundred kilometers, could have occurred after the hematite units were deposited. More importantly, the large amount of erosion that has occurred in this region makes it unlikely that the remains of the original bounding topography of a closed basin would be preserved today. An excellent example of the large-scale erosion that has occurred in this region can be seen by the presence of several large, circular occurrences of Ph standing as elevated mesas (Figure 5). These units were likely deposited within large (tens of kilometer diameter) craters, and the crater walls that originally bounded them have been completely eroded away (e.g., Figure 5), producing an inverted topography of highstanding circular mesas.

4. Summary and Predictions for the MER Rovers

[55] In summary, the three leading candidates for the formation of the hematite-bearing unit in Meridiani Planum all have shortcomings to varying degrees. The model of oxidation of volcanic ash suffers from the poor spectral fit to a magnetite precursor, the dissimilarities of the hematite unit to proposed ash deposits elsewhere, and the spectral dissimilarity between volcanic ash and basaltic sediments. The hydrothermal alteration model suffers primarily from the need to reconcile the very confined vertical extent of the hematite layer over huge distances and across disconnected occurrences. A model of the deposition of precursor Fe oxyhydroxides in water-filled basins requires minor erosion or tilting in order to account for the present-day lack of a completely closed basin for the main Ph unit. We favor this model of deposition in standing water, however, because it does account for the following observations: (1) the occurrence of a thin hematite unit over an area $\sim$150,000 km^2 in size with sharp upper (and possibly lower) contacts; (2) spectral evidence for goethite as a precursor to hematite; (3) the presence of a finely layered, friable texture on Ph in distinct contrast to the morphology of the Etched units on which is lies; (4) embayment relationships on the southern margin of Ph; (5) the occurrence of remnants of hematite-bearing units within isolated craters surrounding of the main Ph unit, and the lack of these units on the intracrater plains; (6) the lack of other hydrothermal minerals; (7) the presence of low-albedo, coarse-grained basalt, rather than ash, as the major component of the hematite-bearing unit; and (8) the differences in morphology between Ph and proposed ash units.

[56] Crystalline hematite is currently exposed only in Meridiani, Aram Chaos, and a few locations within Valles Mariners [*Christensen et al.*, 2001]. Thus the formation of hematite-bearing material appears to have required a specific set of conditions that may have occurred only rarely through Mars history. The occurrence of unweathered olivine, pyroxene, and feldspar in basalts throughout the equatorial region provides strong evidence that extensive aqueous weathering has not occurred on Mars [*Christensen et al.*, 2000a, 2003a; *Hoefen et al.*, 2003]. Thus the presence of a small number of bodies of standing water appears to represent brief, localized phenomena set against the backdrop of a cold, frozen planet.

[57] It is expected that in situ observations from the MER Opportunity rover will address some of these questions. The origin of hematite from oxidation of ash would be supported by observations from microscopic and panoramic imaging of the rock and sediment textures indicative of ash and by the detection of precursor magnetite or partially hematitzed magnetite grains using infrared and Mössbauer spectroscopy [*Squyres et al.*, 2003]. A hydrothermal origin can be tested using the Miniature Thermal Emission Spectrometer [*Christensen et al.*, 2003b] and Mössbauer spectrometer to look for other associated hydrothermal minerals, and microscopic images can be used to determine if the hematite occurs along grain boundaries and in veinlets indicative of postdepositional fluid migration and alteration. The origin of hematite in water-filled basins can be tested by looking for large- and small-scale sedimentary structures. Mineralogic, elemental, or textural evidence can be used to detect a precipitated hematite precursor, such as goethite, that was deposited as a continuous layer, rather than from a later hydrothermal fluid. Rounded grains or hematite/Fe oxyhydroxide spheroids would be compelling evidence for this model. In addition, the occurrence of coarse-grained basalt as a major component and as a sedimentary, rather than a primary, igneous component can be used to distinguish a sedimentary versus volcanic origin.

[58] **Acknowledgments.** We wish to thank the engineers at Raytheon Santa Barbara Remote Sensing for the development of a superb THEMIS instrument, the engineers at Lockheed Martin Astronautics for the development and operation of an excellent Odyssey spacecraft, and the engineers and scientists at the Jet Propulsion Laboratory for the operation of the highly successful Odyssey mission. We thank the ISIS Software Development Team at the U.S.G.S. in Flagstaff, AZ, led by Jim Torson for the development of the ISIS geometry software, and the THEMIS mission operations and software development groups at Arizona State University, led by Greg Mehall, Noel Gorelick, Kelly Bender, Laural Cherednik, Andras Dombovari, and Kim Murray for the excellent operation of the THEMIS investigation. Noel Gorelick, Michael Weiss-Malik, and Ben Steinberg led the development of the JMARS data analysis software used extensively in this study. Noel Gorelick produced the mosaics used in Figures 1 and 2. We thank Tim Glotch, Dick Morris, Trevor Graff, and Mike Wyatt for helpful discussions. Detailed reviews by Brian Hynek and Jeffery Moore significantly improved this manuscript. This work was supported by the 2001 Mars Odyssey Science Office and the Mars Global Surveyor Science Office.

References

Arvidson, R. E., F. P. Seelos IV, K. S. Deal, N. O. Snider, J. M. Kieniewicz, B. M. Hynek, M. T. Mellon, and J. B. Garvin (2003), Mantled and exhumed terrains in Terra Meridiani, Mars, *J. Geophys. Res.*, *108*(E12), 8073, doi:10.1029/2002JE001982.

Bandfield, J. L. (2002), Global mineral distributions on Mars, *J. Geophys. Res.*, *107*(E6), 5042, doi:10.1029/2001JE001510.

Bandfield, J. L., V. E. Hamilton, and P. R. Christensen (2000), A global view of Martian volcanic compositions, *Science*, *287*, 1626–1630.

Berner, R. A. (1969), Goethite stability and the origin of red beds, *Cosmochim. Acta.*, *33*, 267–273.

Bischoff, J. L. (1969a), Goethite-hematite stability relations with relevance to sea water and the Red Sea brine system, in *Hot Brines and Recent*

Heavy Metal Deposits in the Red Sea, edited by E. T. Degens and D. A. Ross, pp. 402–406, Springer-Verlag, New York.

Bischoff, J. L. (1969b), Red Sea geothermal brine deposits: Their mineralogy, chemistry, and genesis, in *Hot Brines and Recent Heavy Metal Deposits in the Red Sea*, edited by E. T. Degens and D. A. Ross, pp. 368–401, Springer-Verlag, New York.

Bookstrom, A. A. (1995), Magmatic features of iron-ores of the Kiruna type in Chile and Sweden—Ore textures and magnetite geochemistry—A discussion, *Econ. Geol.*, *90*, 469–473.

Burns, R. G. (1993), Rates and mechanisms of chemical weathering of ferromagnesian silicate minerals on Mars, *Geochim. Cosmochim. Acta*, *57*, 4555–4574.

Butuzova, G. Y., V. A. Drits, A. A. Morozov, and A. I. Gorschov, (1990), Processes of formation of iron-manganese oxyhydroxides in the Atlantic-II and Thetis Deeps of the Red Sea, in *Sediment-Hosted Mineral Deposits*, edited by J. Parnell, Y. Lianjun, and C. Changming, *Spec. Publ. Int. Assoc. Sedimentol.*, *11*, 57–72.

Catling, D. C., and J. M. Moore (2003), The nature of coarse-grained crystalline hematite and its implications for the early environment of Mars, *Icarus*, *165*, 277–300.

Christensen, P. R., J. L. Bandfield, M. D. Smith, V. E. Hamilton, and R. N. Clark (2000a), Identification of a basaltic component on the Martian surface from Thermal Emission Spectrometer data, *J. Geophys. Res.*, *105*, 9609–9622.

Christensen, P. R., et al. (2000b), Detection of crystalline hematite mineralization on Mars by the Thermal Emission Spectrometer: Evidence for near-surface water, *J. Geophys. Res.*, *105*, 9623–9642.

Christensen, P. R., M. C. Malin, R. V. Morris, J. L. Bandfield, and M. D. Lane (2001), Martian hematite mineral deposits: Remnants of water-driven processes on early Mars, *J. Geophys. Res.*, *106*, 23,873–23,885.

Christensen, P. R., et al. (2003a), Morphology and composition of the surface of Mars: Mars Odyssey THEMIS results, *Science*, *300*, 2056–2061.

Christensen, P. R., et al. (2003b), Miniature Thermal Emission Spectrometer for the Mars Exploration Rovers, *J. Geophys. Res.*, *108*(E12), 8064, doi:10.1029/2003JE002117.

Edgett, K. S., and T. J. Parker (1997), Water on early Mars: Possible subaqueous sedimentary deposits covering ancient cratered terrain in western Arabia and Sinus Meridiani, *Geophys. Res. Lett.*, *24*, 2897–2900.

Fergason, R. L., and P. R. Christensen (2003), Thermal inertia using THEMIS infrared data, *Lunar Planet. Sci.*, *XXXIV*, abstract 1785.

Fernández-Remolar, , J. Gómez-Elvira, F. Gómez, E. Sebastian, J. Martíin, J. A. Manfredi, J. Torres, C. G. Kesler, and R. Amils (2004), The Tinto River, an extreme acidic environment under control of iron, as an analog of the Terra Meridiani hematite site of Mars, *Planet. Space Sci.*, *52*, 239–248.

Frey, H. V. (2003), Buried impact basins and the earliest history of Mars, in *Sixth International Conference on Mars* [CD-ROM], abstract 1979, Lunar and Planet. Inst., Houston, Tex.

Glotch, T. D., R. V. Morris, T. G. Sharp, and P. R. Christensen (2003), Characterization of the effects of precursor mineralogy on hematite spectra: Application to Martian hematite mineralization, *Lunar Planet. Sci.*, *XXXIV*, abstract 2008.

Glotch, T. D., R. V. Morris, P. R. Christensen, and T. G. Sharp (2004), Effect of precursor mineralogy on the thermal infrared emission spectra of hematite: Application to Martian hematite mineralization, *J. Geophys. Res.*, *109*, E07003, doi:10.1029/2003JE002224.

Hoefen, T., R. N. Clark, J. L. Bandfield, M. D. Smith, J. C. Pearl, and P. R. Christensen (2003), Discovery of olivine in the Nili Fossae region of Mars, *Science*, *302*, 627–630.

Hynek, B. M., and R. J. Phillips (2001), Evidence for extensive denudation of the Martian highlands, *Geology*, *29*, 407–410.

Hynek, B. M., R. E. Arvidson, and R. J. Phillips (2002), Geologic setting and origin of Terra Meridiani hematite deposit on Mars, *J. Geophys. Res.*, *107*(E10), 5088, doi:10.1029/2002JE001891.

Hynek, B. M., R. J. Phillips, and R. E. Arvidson (2003), Explosive volcanism in the Tharsis region: Global evidence in the Martian geologic record, *J. Geophys. Res.*, *108*(E9), 5111, doi:10.1029/2003JE002062.

Johnston, J. H., and D. G. Lewis (1983), A detailed study of the transition of ferrihydrite to hematite in an aqueous solution at 92°C, *Geochim. Cosmochim. Acta*, *47*, 1823–1831.

Krapez, B., M. E. Barley, and A. L. Pickard (2003), Hydrothermal and resedimented origins of the precursor sediments to banded iron formation: Sedimentological evidence from the Early Paleoproterozoic Brockman Supersequence of Western Australia, *Sedimentology*, *50*, 979–1011, doi:10.1046/j.1365-3091.2003.0594.

Lane, M. D., R. V. Morris, S. A. Mertzman, and P. R. Christensen (2002), Evidence for platy hematite grains in Sinus Meridiani, Mars, *J. Geophys. Res.*, *107*(E12), 5126, doi:10.1029/2001JE001832.

Lane, M. D., P. R. Christensen, and W. K. Hartmann (2003), Utilization of the THEMIS visible and infrared imaging data for crater population studies of the Meridiani Planum landing site, *Geophys. Res. Lett.*, *30*(14), 1770, doi:10.1029/2003GL017183.

Langmuir, D. (1971), Particle size effect on the reaction goethite = hematite + water, *Am. J. Sci.*, *271*, 147–156.

Malin, M. C., and K. S. Edgett (2003), Evidence for persistent flow and aqueous sedimentation on early Mars, *Science*, *302*, 1931–1934.

Mellon, M. T., B. M. Jakosky, H. H. Kieffer, and P. R. Christensen (2000), High resolution thermal inertia mapping from the Mars Global Surveyor Thermal Emission Spectrometer, *Icarus*, *148*, 437–455.

Melosh, H. J. (1989), *Impact Cratering, A Geologic Process*, 78 pp., Oxford Univ. Press, New York.

Moore, J. M., A. D. Howard, W. E. Dietrich, and P. M. Schenk (2003), Martian Layered Fluvial Deposits: Implications for Noachian Climate Scenarios, *Geophys. Res. Lett.*, *30*(24), 2292, doi:10.1029/2003GL019002.

Morris, R. V., M. D. Lane, S. Mertzman, T. D. Shelfer, and P. R. Christensen (2000), Chemical and mineralogical purity of Sinus Meridiani hematite, *Lunar Planet. Sci.* [CD-ROM], *XXXI*, abstract 1618.

Newsom, H. E., C. A. Barber, T. M. Hare, R. T. Schelble, V. A. Sutherland, and W. C. Feldman (2003), Paleolakes and impact basins in southern Arabia Terra, including Meridiani Planum: Implications for the formation of hematite deposits on Mars, *J. Geophys. Res.*, *108*(E12), 8075, doi:10.1029/2002JE001993.

Parak, T. (1975), Kiruna type ores are "intrusive-magmatic ores of the Kiruna type", *Econ. Geol.*, *70*, 1242–1248.

Phillips, R. J., et al. (2001), Ancient geodynamics and global-scale hydrology of Mars, *Science*, *291*, 2587–2591.

Presley, M. A., and R. E. Arvidson (1988), Nature and origin of materials exposed in the Oxia Palus-Western Arabia-Sinus Meridiani region, Mars, *Icarus*, *75*, 499–517.

Presley, M. A., and P. R. Christensen (1997), Thermal conductivity measurements of particulate materials: 2. Results, *J. Geophys. Res.*, *102*, 6551–6566.

Ramsey, M. S., and P. R. Christensen (1998), Mineral abundance determination: Quantitative deconvolution of thermal emission spectra, *J. Geophys. Res.*, *103*, 577–596.

Ruff, S. W., and P. R. Christensen (2002), Bright and dark regions on Mars: Particle size and mineralogical characteristics based on Thermal Emission Spectrometer data, *J. Geophys. Res.*, *107*(E12), 5127, doi:10.1029/2001JE001580.

Schmalz, R. A. (1959), A note on the system Fe_2O_3-H_2O, *J. Geophys. Res.*, *64*, 575–579.

Smith, D. E., et al. (2001), Mars Orbiter Laser Altimeter: Experiment summary after the first year of global mapping of Mars, *J. Geophys. Res.*, *106*, 23,689–23,722.

Squyres, S. W., et al. (2003), Athena Mars rover science investigation, *J. Geophys. Res.*, *108*(E12), 8062, doi:10.1029/2003JE002121.

Tunell, G., and E. Posnjak (1931), The stability relations of goethite and hematite, *Econ. Geol. Bull. Soc. Econ. Geol.*, *26*(3), 337–343.

Vorobyeva, K. A., and Y. P. Melnik (1977), An experimental study of the system of Fe_2O_3-H_2O at T = 100–200°C and P up to 9 kilobars, *Geochem. Int.*, *8*, 108–115.

Wefers, K. (1966), On the system Fe_2O_3-H_2O. Part 1, *Deutsch. Keram. Ges.*, *43*, 677–702.

P. R. Christensen and S. W. Ruff, Department of Geological Sciences, Campus Box 6305, Arizona State University, Tempe, AZ 85287-6305, USA. (phil.christensen@asu.edu)